



Published in final edited form as:

Dalton Trans. 2013 May 7; 42(17): 5985–5998. doi:10.1039/c2dt32174b.

Characterization of a versatile organometallic pro-drug (CORM) for experimental CO based therapeutics

João D. Seixas^{1,†}, Abhik Mukhopadhyay^{2,†}, Teresa Santos-Silva², Leo E Otterbein³, David J. Gallo³, Sandra S. Rodrigues¹, Bruno H. Guerreiro¹, Ana M. L. Gonçalves¹, Nuno Penacho¹, Ana R. Marques¹, Ana C. Coelho⁴, Patrícia M. Reis⁴, Maria J. Romão², and Carlos C. Romão^{1,4,*}

¹Alfama Lda, Taguspark, núcleo central 267, 2740-122 Porto Salvo, Portugal

²REQUIMTE, Departamento de Química, Faculdade de Ciências e Tecnologia, Universidade Nova de Lisboa, 2829-516 Caparica, Portugal

³Harvard Medical School, Department of Surgery, Transplant Institute, Department of Surgery, Beth Israel Deaconess Medical Center, Boston, MA 02215

⁴Instituto de Tecnologia Química e Biológica da Universidade Nova de Lisboa, Av. da República, EAN, 2780-157 Oeiras, Portugal

Abstract

The complex *fac*-[Mo(CO)₃(histidinate)]Na has been reported to be an effective CO⁻ Releasing Molecule *in vivo*, eliciting therapeutic effects in several animal models of disease. The CO releasing profile of this complex in different settings both *in vitro* and *in vivo* reveals that the compound can readily liberate all of its three CO equivalents under biological conditions. The compound has low toxicity and cytotoxicity and is not hemolytic. CO release is accompanied by a decrease in arterial blood pressure following administration *in vivo*. We studied its behavior in solution and upon the interaction with proteins. Reactive oxygen species (ROS) generation upon exposure to air and polyoxomolybdate formation in soaks with lysozyme crystals were observed as processes ensuing from the decomposition of the complex and the release of CO.

Introduction

The use of CO Releasing Molecules (CORMs) to deliver therapeutically useful amounts of CO *in vivo* is now well established and has been recently reviewed.^{1,2} This CO delivery process is triggered by a chemical or biological event that takes place *in vivo*, after administration, and its nature depends on the chemistry and reactivity of the CORM. One of the most important advantages assigned to the administration of such pro-drugs is the possibility of controlling, targeting, and hopefully minimizing the amount of CO in circulation. The main disadvantage is that like any other pro-drug, the release of the active principle, CO in this case, from a molecular scaffold produces metabolites, which must be toxicologically safe. Among all molecules that are able to undergo decarbonylation, that is, to lose CO upon decomposition, transition metal carbonyls [M(CO)_xL_y]^{±z} (M = transition

*Corresponding Author. ccr@itqb.unl.pt.

†as joint first author

Notes

J. D. Seixas, L. E Otterbein, D. J. Gallo, S. S. Rodrigues, B. H. Guerreiro, A. M. L. Gonçalves, N. Penacho, A. R. Marques, P.M. Reis and C. C. Romão worked for and hold financial interests in Alfama Inc.

Supplemental information

Supporting information is available. Table S1–4 and Figure S1–5. See DOI PDB ID code: 4B1A

metal; L = ancillary ligand; z = charge) have proved to be the more versatile ones.³ In this area, two *fac*-[Ru^{II}(CO)₃L₃] derivatives have played a prominent role: DMSO soluble [Ru(CO)₃Cl₂]₂ (CORM-2)⁴ and its water soluble derivative [Ru(CO)₃Cl(κ²-H₂NCH₂CO₂)] (CORM-3).⁵ In fact, a very large number of *in vitro* and *ex vivo* studies using these complexes resulted in biological and physiological effects attributed to CO. More remarkable though is the broad range of beneficial therapeutic effects obtained *in vivo* in many animal models of disease pathology (see references ^{1, 2} and refs therein). One of the most striking observations in these *in vivo* studies is that such molecules are effective at doses where the values of carboxyhemoglobin (COHb) levels in the blood are unchanged (*ca.* 2–5%) or only slightly above baseline.^{6, 7} Although these CORMs exert biological effects without changing COHb, we believe that the active molecule is CO because once such CORMs are depleted from labile CO, by simple aging in solution, their therapeutic efficacy is lost. However, the mechanism of CO release and delivery from these CORMs has remained elusive since they do not release measurable amounts of CO when solubilized and react rapidly with plasma proteins, e.g. serum albumin, without releasing CO. Instead, they form protein-Ru^{II} (CO)₂ adducts and release CO₂.⁸

In contrast to this stealth mode of CO transport and delivery, CO inhalation produces dose dependent, highly predictable amounts of COHb in circulation, which can be correlated to the biologic effects. Although higher values of COHb in systemic circulation should be avoided to prevent toxicity, they are useful in experimental animal models of disease precisely because, at least in principle, they help identify positive therapeutic responses to exogenous CO while allowing precise pharmacokinetic and pharmacodynamics evaluation.

Based on the simplicity of administration of a small, water soluble organic compound,^{2, 3} we decided to develop a CORM that would somehow mimic inhalation and deliver CO to the organism in response to a decomposition trigger. As with CO inhalation, no tissue specificity can be expected from this approach. However, one may expect the administration of a bolus of such a CORM to result in a controllable, dose-dependent amount of CO to be present in the circulation and allow a correlation with therapeutic efficacy. One of the objectives of these attempts would be to see if controlled decomposition of metal carbonyl complexes would mimic the therapeutic effects of CO inhalation. Another would be to probe the therapeutic action of CO in many animal models of disease using CORM technology instead.

In this setting, the rationale for the choice of the known histidinate complex *fac*-[Mo(CO)₃(histidinate)]Na as a leading experimental CORM is simple.⁹ The complex is readily prepared and purified. It is soluble and stable in water under an inert atmosphere but decomposes in solution in the presence of oxygen. Therefore, this complex is expected to release CO immediately after peritoneal or intravenous administration by virtue of the decomposition triggered by molecular oxygen. As with CO inhalation, CO released from this complex is transported in the systemic circulation, bound or unbound to Hb, and carried and distributed to the tissues. The lack of toxicity of the only ancillary ligand, histidine, and the expected low toxicity of molybdenum metabolites further supported the design of such a compound.^{10–12} This CORM, also known as ALF186, proved to be a useful experimental tool in CO therapy, being curative in a number of disease models. Gastric ulcer protection from NSAIDs,¹³ inflammatory bowel disease,¹⁴ and more recently neuroprotection against microglia induced inflammation are reported examples.¹⁵ The related complex [Mo(CO)₂(η³-allyl)(histidinate)] is very stable in biological media and has been derivatized to label the neuropeptide [Leu⁵]-enkephalin.¹⁶

Very recently, the complex $[\text{Mn}(\text{CO})_3(\text{histidinate})]$, isoelectronic with ALF186, has been shown to be stable under biological conditions, releasing CO only upon activation with light.¹⁷ This property classifies $[\text{Mn}(\text{CO})_3(\text{histidinate})]$ as a photoCORM.¹⁸

In the following, we describe the characterization of the experimental CORM $[\text{Mo}(\text{CO})_3(\text{histidinate})]\text{Na}$ (ALF186) in what regards its CO release profile, and the fate of its interactions with key proteins like serum albumin and hemoglobin (Hb), which are of fundamental importance to guide the design of CORMs with pharmacologically acceptable ADME (administration, distribution, metabolism and excretion) profiles. The interaction with HEWL, lysozyme crystals provided the means to probe the nature of the decomposition products that result from the aerobic decomposition of ALF186 in biological compatible media.

Results

Synthesis, stability and oxidative decarbonylation

The complex *fac*- $[\text{Mo}(\text{CO})_3(\text{histidinate})]\text{Na}$, (ALF186) is an octahedral, zerovalent Mo complex with the structure shown in Figure 1.

It can be prepared as a yellow crystalline solid in multi-gram scale (75% yield) by refluxing $\text{Mo}(\text{CO})_6$ with histidine and NaOH in THF:H₂O (15:2) overnight. In the solid state, kept under nitrogen, at room temperature (rt) and in the dark, ALF186 was found to be stable for three months, as judged by ¹H NMR, FTIR and elemental analysis. When kept under nitrogen at room temperature it was also found to be stable up to two months under standard illumination conditions.^{19, 20} Visual inspection suggests it remains stable for longer periods under these conditions but no analytical control was performed above three months.

Remarkably, the crystalline compound is stable for two months under normal air, at room temperature (rt) and in the dark. No tests were done under the simultaneous action of light and air.

In contrast to its unexpectedly high stability as a solid, ALF186 decomposes readily when dissolved in aqueous solvents under normoxic conditions. This decomposition is accompanied by liberation of CO, which was quantified by GC in the headspace of the solution using a Thermal Conductivity Detector against a calibration curve for CO (see Experimental section).

When ALF186 is dissolved in deoxygenated aqueous media under an atmosphere of nitrogen, at 37°C essentially no CO is liberated and the number of equivalents of CO in the headspace is typically zero or a value ≈ 0.1 equiv. (see Supporting Information, Table S1 and S2). On the contrary, in similar tests done under normoxic conditions, that is, with non-degassed solutions and vessels, the amount and rate of CO released to the headspace is very significant. After 0.5h *ca.* 1 equivalent of CO has been liberated and after 4h a ceiling of *ca.* 2.6 equivalents of CO is already attained. This profile holds for several aqueous media (see SI, Tables S1, S2, S4) but has a slight variation with pH, being *ca.* 50% slower at the acidic pH values (2.5) to be found in the stomach (see SI, Table S3). The absolute value obtained varies with slightly different experimental conditions that have a direct influence on the oxygenation of the sample (e.g. headspace volume, sample concentration). No improvement in the precision and accuracy of these measurements was deemed necessary since they clearly show the essence of the profile of CO release of the compound and its trigger: molecular oxygen (O₂).

Therefore, ALF186 will start releasing CO into the circulating blood and other tissues shortly after being administered intravenously (i.v.), intraperitoneally, (i.p.) or even orally. This classifies ALF186 as an oxygen activated (triggered) CORM, which replaces inhalation of CO by delivery from a molecular entity administered either as a solid or as an injectable solution (see below actual *in vivo* COHb data).

ALF186 reduces hemoglobin, myoglobin and cytochrome c

Hemoproteins have an important redox chemistry, which is connected to the oxidation states of the central iron ion of the heme. Since different oxidation states of the heme iron correspond to different reactivities and biological outcomes, the regulation of these heme oxidation states has important physiological consequences.²¹ Being an electron-rich, reducing complex ALF186 is likely to interfere with this regulation. Indeed, treatment of oxidized horse heart muscle cytochrome *c* (cyt*c*) solutions with ALF186 leads to the instantaneous formation of reduced cyt*c* (ferrocyanochrome *c*) as can be seen by the UV-Vis spectra (see SI Figure S1a). CO gas alone or the widely used Ru(II) CORM-3 are unable to make this reduction (see SI Figure S1b).

Both oxidized hemoglobin (met-Hb) and oxidized myoglobin (met-Mb) are also instantaneously reduced by ALF186. The reduced protein immediately picks-up the CO that is released from oxidized ALF186 with concomitant formation of COHb (or COMb) as can be seen in the UV-Vis spectra by the shift of the Soret bands and the formation of the Q bands due to CO coordination, which are absent in the initial spectrum of the oxidized proteins (See SI, Figure S1c and S1d). CO gas cannot effect such reductions and CORM-3 is unable to reduce met-Mb (SI, Figure S1e). Very recently it was shown that CORM-3 cannot even carbonylate deoxy-Mb or oxy-Hb.²²

Interaction with whole blood in vitro: COHb elevation

The addition of ALF186 to sheep blood at 37°C followed by the immediate oximetric quantification of COHb originated the data collected in Table 3. In agreement with the reducing ability of ALF186 documented in the preceding section, oximetry reveals the total absence of met-Hb. However, the most striking and unexpected information in Table 1 is the number of equivalents of CO that were liberated from ALF186 at “time zero”, that is, the time of mixing and measuring. In fact, all three equivalents of CO were “instantaneously” delivered from ALF186 to blood Hb under normoxic conditions in a bolus like manner. This is much faster than the release of CO measured by GC in aqueous solutions (Table S1 – S4). One possible explanation is that the plasma proteins have significantly accelerated the release of CO from ALF186. The ratio ALF186: serum albumin in these experiments is *ca.* 1:1 since the blood is acquired diluted (1:1) in Alsever’s solution (see Sigma A3551 for a definition of Alsever’s). Alternatively, the scavenging effect of Hb is the real cause of this rapid loss of CO (see below).

In contrast, CORM-3 does not raise the value of COHb under similar conditions up to 2h.⁸

Interaction with Human Serum Albumin

The acceleration of CO release from ALF186 that takes place in blood prompted a first screening of the interaction of the compound with serum albumin, which is the most abundant protein in blood plasma (60% of the total plasma protein) and functions as a transporter both to endogenous and exogenous compounds. Moreover, it is well known that the interaction of small molecule drugs with plasma proteins plays an important role in the distribution of the drug in the body and affects properties like toxicity and biological activity by changing several ADME parameters and pharmacokinetics.^{23, 24} These effects may even

be more important in metal based drugs and pro-drugs which can be drastically modified upon interaction with proteins as we and others have recently shown.^{8, 25}

The UV-Vis spectrum of an anaerobic solution of ALF186 (250 μ M) shows a slow decay but no important new features are apparent (SI, Figure S3a). Similar spectra taken in the presence of HSA (ALF186:HSA = 5:1) also reveal minor initial variations namely the appearance of a small, ill defined absorption at 386 nm which stops growing *ca.* 1h after incubation and remains unchanged up to 4h (SI, Figure S3a). Experiments using ALF186 and acid free BSA in a 40:1 or 5:1 molar ratio under nitrogen, did not reveal release of either CO or CO₂ up to 4h incubation time at rt. Since we are not expecting a large difference in reactivity between HSA and BSA we can conclude that the small interaction between HSA and ALF186 that exists under anaerobic conditions does not induce CO release from the complex.

As mentioned above, when ALF186 is dissolved in PBS buffer at pH7.4 under normoxic conditions a fast and extensive release of CO is observed. Unfortunately, the variation of the UV-Vis spectra of such solution with time doesn't identify any clear process or intermediates (Figure 2a). However, when ALF186 is incubated with HSA (5:1 ratio) in normoxic conditions in PBS buffer at pH7.4 more evident changes take place, as shown in the Figure 2b.

Immediately after mixing (t_0) the absorbance of the peak at 308 nm is much higher than the absorbance of ALF186 alone at this wavelength and concentration. This shows that new species are readily formed upon mixing ALF186 and HSA in the presence of O₂, which then decay as shown in Figure 2b (inset).

A new band is observed at 386 nm within 10 min of incubation, which stops increasing in absorbance after *ca.* 1h. Qualitatively, this spectral variation at 386 nm seems similar to that observed in the incubation under nitrogen (Figure S3a), but the absorbance is higher under air at the same initial concentrations of ALF186 and HSA. These data to indicate that HSA interacts with ALF186 under O₂ in a different manner than it does under N₂. Importantly, however, this interaction is not responsible for the acceleration of CO release. Independent experiments with ALF186 and BSA in a 5:1 molar ratio under air show that the rate of CO release is slightly retarded in the presence of BSA at similar values of [ALF186] and headspace volume as shown in Figure 3.

Therefore, the acceleration of CO release in blood is not due to the presence of serum albumin but is most likely due to the scavenging action of Hb.

Interaction with the model protein HEWL (hen egg white lysozyme): X-ray crystallography

Since the above data suggest the presence of an interaction between HSA and ALF186 we attempted to go further into the clarification of these new entities by means of X-ray crystallography. However, in spite of multiple attempts we were unable to obtain any useful crystallographic data from the experiments of co-crystallization of HSA and ALF186. Therefore, we turned to the study of the interaction of ALF186 with crystals of the model protein HEWL (hen egg white lysozyme).

The HEWL crystals soaked with ALF186 diffracted up to 1.7 \AA resolution, and belong to the same space group ($P4_32_12$) as the native HEWL structure (pdb code 193L). Apart from the protein moiety there is a sodium and a chloride ion present in the structure. After detailed structure analysis, no metal atom was found bound to the usual metal binding sites of lysozyme (histidines, aspartates or arginines at the protein surface) as observed in the numerous lysozyme-metal structures deposited in the PDB. However, a site with strong

electron density was found near loop 43–48 and modeled as the well characterized polyoxomolybdate cluster $[\text{PMo}_{12}\text{O}_{40}]^{3-}$, also known as Keggin's ion. The cage shaped structure of the molybdenum cluster is sitting on the fourfold axis, surrounded by three other symmetry related molecules of lysozyme. The cluster is hydrogen bonded to the Arg45 residue via one of the terminal oxygen atoms. The presence of the molybdenum atoms was confirmed by calculating an anomalous map (Figure 4). Even though the diffraction data were collected far from the molybdenum K edge, the large peaks obtained facilitated positioning the cluster and only six molybdenum atoms are present in the asymmetric unit. Even though the electron density for all 40 oxygen atoms is not well defined, it is very clear for the phosphorus atom, located in the center of the cluster. Although we did not use phosphate to prepare the crystallization buffer, the phosphate ion present in the water used for crystallization experiment and the acidic nature of the solution (pH~4.5) helped to form the polyoxomolybdate cluster in the crystal. The homogeneous B-factor variance of all the atoms of the cluster indicates the quality of fit. The blue coloration after soaking is consistent with the cluster being partially reduced.

The FTIR spectrum of crystals of HEWL soaked with ALF186 (ground and deposited on KBr pellets) shows bands at around 820 cm^{-1} , corresponding to the Mo-O-Mo stretching and does not show the characteristic Mo-CO bands at *ca.* 2000 cm^{-1} , as observed for protein-CORM-3 adducts.⁸ These results confirm that all CO has been released from ALF186 upon its interaction with the protein and reveals that the initially zerovalent molybdenum atom is oxidized to the heteropolyoxomolybdate cluster during its interaction with the protein in normoxic atmosphere. This crystallographic data provides circumstantial evidence for the type of metal metabolites that are expected to form from this kind of zerovalent molybdenum CORMs in acidic solution. At higher values of pH the degree of polymerization is likely to be different and other clusters may be favored. Importantly, though, is the fact that such clusters or oligomers do not form covalent bonds to the surrounding protein chains.

To the best of our knowledge this is the first structural example of the interaction of a $[\text{PMo}_{12}\text{O}_{40}]^{3-}$ cluster with a protein. The tungsten analog of Keggin's ion has been found in the crystal structure of human small CTD-phosphatase protein.²⁶ Another isopolymolybdate cluster consisting of seven molybdenum atoms has been found in the structure of CitAperiplasmic sensor domain protein.²⁷

The cytotoxicity of ALF186 was evaluated in 3 cell lines: a liver cell line – HepG2; a kidney cell line – LLC-PK1; and a macrophage cell line – RAW264.7. ALF186 was tested up to a concentration of $100\text{ }\mu\text{M}$. ALF186 showed no toxicity to LLC-PK1 and RAW264.7 cells after 24 h incubation (Figure 5). However, some toxicity was observed on the human liver cells HepG2. ALF186 at a concentration of $100\text{ }\mu\text{M}$ reduced the survival of HepG2 cells by approximately 30%.

In vivo toxicity

The *in vivo* toxicity of ALF186 was tested in healthy mice. No gross abnormalities in behavior, as well as in the external or internal organs were observed in mice that were treated for up to 40 days with ALF186 in PEG300/water (1:4) with daily i.p. injections of 20 mg/kg . At 137.5 mg/kg (i.p.) no signs of toxicity were observed. Acute toxicity was observed at a dose of 500 mg/kg administered intraperitoneally. This dose, much higher than that needed for therapeutic action in most disease models tested, and still safe when administered orally (see Figure 6b), caused death after *ca.* 8 min post injection. The values of %COHb were above the higher scale limit of the oximeter (70%).

Hemolysis

In order to be a useful molecule, even at the experimental level, a CORM must avoid the deleterious effects of hemolysis. Moreover, the control read-out of blood COHb may be altered upon release of free Hb in circulation by RBC hemolysis.

The hemolytic index of ALF186 was evaluated using sheep RBC and the compound was found to be not hemolytic at concentrations up to 1 mg/mL (Figure S4 in SI). Note that this concentration is *ca.* 8 times higher than the concentration used in the *in vitro* experiments with whole blood, summarized in Table 1.

COHb elevation in vivo

The kind of “bolus like” delivery of CO seen in the *in vitro* test with sheep blood was confirmed with administration of ALF186 to mice *in vivo*. As can be seen in Figure 6a, i.p. administration of ALF186 at doses of 20 or 40 mg/kg to Balb/C mice, led to the increase in COHb to 15% and 25%, respectively, within 10–15 min. COHb steadily decreases thereafter returning to baseline values within 3h. The values of COHb measured at the peak correspond to those expected for the delivery of an amount of CO corresponding to the three equivalents of CO carried in the injected dose (bolus). When ALF186 was administered orally, the rise in COHb was much slower with a more prolonged plateau of elevated COHb (Figure 6b). Indeed, when 500 mg/kg of ALF186 are administered orally, the COHb levels peaked at 50–70 min with the maximum COHb levels reaching 35–40%, which correspond to roughly one half of those obtained by i.p. administration at the same dose.

Hemodynamic effects of inhaled CO and ALF 186, in anesthetized mice

We next compared the effects of ALF186 and inhaled CO on hemodynamics. CO is a poor vasorelaxing molecule, unlike nitric oxide. Figure 7 shows the results of a direct comparison between inhaled CO (iCO) at 250 ppm continuously versus ALF186 (20 mg/kg, i.p.) in mice. Air control animals were treated exactly the same as the inhaled CO animals. Mean arterial blood pressure (MABP) was measured continuously through a femoral artery catheter. The %COHb was measured at t₀, 10, 60 and 120 min after the start of administration of gas or ALF186. N=3–5 animals/group. Results are mean ± SD of 3–5 animals/group. We observed a rapid increase in COHb in animals treated with ALF186 within 10 min unlike inhaled CO, which was much slower. The rapid increase in COHb in the ALF186-treated mice was accompanied by a rapid decline in MABP that was not observed in air or inhaled CO treated mice. We speculate that the speed of CO entry into the bloodstream elicited either a rapid rise in cGMP as CO binds to the heme protein guanylate cyclase in vascular smooth muscle cells or that ALF186 non-specifically activates a systemic anaphylactic-like response driven by a sudden release of nitric oxide (NO) or histamine. CO is known to be a poor vasodilator unlike NO, but perhaps if COHb levels are increased very rapidly (independent of respiration) the effects on cGMP under these conditions are more dramatic. The MABP returned to baseline levels by 60 min in the ALF186 treated animals. Interestingly, the COHb levels in the single i.p. bolus, ALF186-treated mice did not return to baseline by 120 min suggesting the potential for a slow release of CO from the abdomen into the circulation. Gas-treated animals achieved a steady state COHb as expected, which dissipated with a t_{1/2} of 15 min once the CO administration was stopped.

It is important to note that the active form of ALF186 begins to drop blood pressure and raise COHb 10 min after injection.

Discussion

ALF186: a useful experimental CORM

Our choice of ALF186 as a CORM candidate to deliver CO to tissues intended to explore its instability under oxic conditions to enable the delivery of pre-established amounts of CO at controlled rate following administration to a rodent.

The experimental results reported above confirm this possibility. ALF186 in aqueous media is readily decomposed by atmospheric oxygen (O₂) liberating $\approx 75\%$ of its total CO load (2.26 equivalents), in the dark at 37°C after 2h and 1 equivalent after *ca.* 0.5h. Importantly, under similar anaerobic conditions no CO is released. This reaction is faster at higher pH (Table 2), an observation common to many substitution reactions of complexes with ammine and amine ligands both in carbonyl and Werner type coordination chemistry.^{29, 30} Regardless mechanistic details, which were not investigated, the important finding is that the CO release rate and extension (yield of free CO) from ALF186 is relatively constant in all biological media at pH ≈ 7.4 including those usually used as injectable vehicles for *in vivo* administration (e.g. saline, PBS).

In this manner, ALF186 is classified as an oxygen activated or triggered CORM, which inevitably decomposes and liberates CO in aerobic biological settings. Indeed, the swift release of CO from ALF186 becomes even more impressive when the compound is incubated with sheep whole blood *in vitro*. As seen in Table 1, the release of CO is virtually instantaneous and quantitative as measured by the value of COHb formed. The possibility that this fast reaction is caused by lysis of red blood cells and fast reaction of free Hb with ALF186 is ruled out because the standard test procedures showed that ALF186 is not hemolytic up to 1 mg/mL, a concentration ≈ 8 times higher than the concentration of 0.122 mg/mL used for the COHb measurements in Table 1.

This fast reaction of CO with hemoglobin in the blood *in vitro* translates *in vivo* where we observed a rapid rise in COHb over time following either an oral or intraperitoneal dosing of ALF186 (Figure 6a). Not unexpectedly, oral administration resulted in a much slower increase of COHb as CO is absorbed through the stomach into the circulation. The slower oral delivery probably also reflects the slow rate of CO release observed at pH 2.5 (Table S3) when compared to the instantaneous release in blood which follows *i.p.* administration.

These results show that ALF186 is very effective for the rapid delivery of “solid CO”. Successive administrations or a continuous infusion can modulate overall profiles with extended elevation plateaus of COHb. So, ALF186 is a very useful tool to precisely manipulate levels of CO in the circulation. The favorable characteristics of ALF186 include its low cytotoxicity (Figure 5) and low *in vivo* acute toxicity. Although no full studies of sub-acute toxicity have been deemed necessary, a 40-day long treatment, with daily *i.p.* administration of 20 mg/kg doses of ALF186 to mice did not reveal any gross abnormalities (data not shown).

Due to this versatility, ALF186 has been successively used in several important animal models of disease, including gastric protection from adverse effects of NSAIDs¹³, inflammatory bowel disease¹⁴, vascular injury³¹ and protection against microglia induced neuroinflammation¹⁵ as well as in *in vitro* studies.³²

The reason we classify ALF186 as an experimental CORM stems from the fact that many of its physicochemical properties are far from those usually considered as drug-like in the common pharmacological sense (see reference³ for a discussion on this topic). Rather than achieving a tissue targeted delivery of CO this CORM mimics CO delivery by inhalation

and is not tissue specific. In contrast to ALF186, *fac*- [Ru(CO)₃L₃] complexes like CORM-2 and CORM-3 that have been dominating the literature on CORMs since their introduction by Motterlini, Mann and coworkers in 2002–2003,^{4, 5, 33, 34} do not release CO to the headspace of their solutions, under aerobic or anaerobic conditions. This observation has been carefully quantified for CORM-3 even to very low limits of CO detection,⁸ but is true for CORM-2 and more than ten other related complexes with different L₃ sets of ligands with N, O, S and P donors.³⁵ CORM-2 and CORM-3 produce no COHb elevation after incubation with whole blood *in vitro* or after administration to a rodent *in vivo* yet impart important biological effects. In this manner, they cannot be qualified as CO releasers in the same chemical sense as ALF186.

More importantly though, both types of experimental CORMs, ALF186 and *fac*- [Ru(CO)₃L₃] complexes, with properties that are still far from those of drug-like substances, have produced impressive therapeutic results that have been attributed to their ability to release CO. A detailed understanding of the mode of action of these CORMs is still unclear, but seems to model the data with CO gas.

ALF186: contributions for the study of metal carbonyls in biological conditions

Studies of ALF186 also contributed valuable information towards the development of CO releasing drugs based on metal carbonyl complexes (MCC). Indeed, the rational preparation of such drug-like CORMs requires a deeper knowledge of the reactivity and fate of MCCs in the presence of biological molecules, an area where not much is yet known.³

At the outset of this work we were aware of the susceptibility of ALF186 to oxidation by molecular oxygen (O₂) and we intended to take advantage of this fact to achieve fast delivery of CO into the blood stream. However, these experiments led us to identify an important drawback of this type of initiation of CO release from MCCs: the formation of reactive oxygen species (ROS). In fact, as described elsewhere,³² the use of EPR spectroscopy and a spin trap (BMPO) led to the identification of the formation of hydroxyl radicals ([•]OH) as the sole ROS species emerging from the interaction of ALF186 with O₂. Later studies showed that the formation of HO radicals seems to be a feature of the interaction of several CORMs with O₂ including [Mo(CO)₅Br][NET₄], CORM-2,³⁶ and CORM-3.³² Since the stabilization of the M-CO bonds requires reduced species most MCCs are prone to react with O₂ to generate ROS. Even when they are air stable, like CORM-2 and CORM-3, side reactions may lead to the formation of ROS species as long as O₂ is present.

The easy formation of ROS species and the importance of their biological activity must always be kept in mind when attempting to understand the mechanisms of action of CORMs since ROS are particularly important in cellular signaling and function including those involving CO signaling.³⁷ This, of course, results in a much more difficult interpretation of the biological effects elicited by CORMs as discussed *à propos* the ROS mediated biocide activity of [Mo(CO)₅Br][NET₄] and CORM-2³⁶ and the effects of CORM-2, CORM-3 and several Mo⁰ CORMs in vascular tissues.³²

Another important consequence of the reducing nature of ALF186 and several other CORMs is their capacity to reduce heme proteins and thereby enhancing their affinity for CO. ALF186 proved to be rather active in this context, and, as shown in Figure 2, is able to reduce oxidized cytc, met-Hb and met-Mb. In the case of Hb and Mb this reduction leads to the carbonylation of the protein, which does not happen with CORM-3. Therefore, a compound like ALF186 is a much stronger donor of CO to heme proteins than CORM-3, which was recently shown to be unable to carbonylate even the fully reduced deoxy-Mb, contrary to previous and widespread belief.²² Importantly, the capacity of CORMs to reduce

met-Hb may permit its use in the treatment of injuries resulting in high met-Hb levels. The interaction of ALF186 and CORM-3 with serum albumin (HSA and BSA) also provides an interesting comparison of different reactivity profiles and CO release outcomes from apparently similar metal carbonyl complexes. From the point of view of CO release, ALF186 only seems to have a relevant interaction with albumin under aerobic conditions. Under these conditions the UV-Vis spectrum shows that new species are rapidly formed in solution upon mixing of HSA and ALF186. However, in comparison to an assay in protein free PBS solution, CO release is not affected in the beginning of the reaction but is retarded at longer times at a 5:1 ratio of ALF186 to BSA (Figure 5). Raising this ratio to 41:1 the influence of the presence of BSA is no longer visible (see Supporting Information, Figure S3). The formation of CO₂ is only marginal in the whole process. In contrast, CORM-3 and similar compounds react rapidly with HSA independently of the presence of O₂, to release 1 equivalent CO₂ and form HSA-Ru(CO)₂ adducts that are very slow releasers of CO.^{8, 38–40} Clearly, the reaction of MCCs with serum albumin can lead to quite different results and deserves more careful study. In fact, the interaction of small molecule drugs and metal complexes with serum albumin,⁴¹ are prominent in ADME analysis as well as the pharmacokinetic and pharmacodynamic properties of transition metal based compounds.^{25, 42, 43}

Recent findings on the modulation of the mode of action of the Ru(III) anti-tumoural drug NAMI-A by HSA have just provided another outstanding example of the importance of these interactions.²⁵ It is therefore surprising to realize that studies of the reactivity of metal carbonyl complexes with proteins are very scarce and contemplate only a handful of examples.^{8, 44–46}

The biological influence of the structure of the metal scaffold of a CORM as well as the fate and possible toxicity of the metal products generated by its decomposition are points of major concern that rapidly emerge in any discussion on the use of MCC based CORMs. Two topics assume particular relevance: a) distinguish the biological effects of a CORM from those of its released CO; b) assess the nature of the metal decomposition products. Indeed, beside the biological effects resulting from the release of CO, the scaffold of one CORM may also induce other biological responses, through its structure or the nature of the other ancillary ligands. So, the biological effects due to the release of CO from a CORM should be compared to those obtained in response to the administration of an isostructural complex where the labile CO(s) was replaced with a biologically innocuous ligand like water or chloride. Such control complex would then be called inactivated CORM (iCORM) a concept introduced in the early experiments reported on CORM-3.⁵ and always present in the mind of the biologists experimenting with CORMs.

However, real iCORMs are exceedingly rare due to the fact that the structures stabilized by the CO ligand become very unstable when this ligand is replaced by classical σ -donor ligands like water, amines, halides, and the like. Since, in contrast to CO, such ligands are unable to accept the excess electronic charge of the reduced central ions or atoms of MCCs, their derivatives become very reactive. We believe that the recently reported complexes of formula $[\text{Fe}(\text{CO})(\text{N}5)]^{2+}$ (N5 = pentacoordinated nitrogen ligand) are the first CORMs that have a real iCORM counterpart: the complex $[\text{Fe}(\text{H}_2\text{O})(\text{N}5)]^{2+}$ which readily forms when $[\text{Fe}(\text{CO})(\text{N}5)]^{2+}$ is dissolved in aqueous media.⁴⁷ Most likely, the fast expansion of the field of photoCORMs will produce other examples due to the precise control of the M-CO bond excision resulting from photoactivation.¹⁸

Avoiding these difficulties, iCORMs of experimental CORMs like CORM-3 or ALF186 have been defined as the species generated by dissolving such CORMs in physiological compatible buffer until complete loss of CO release activity of such solutions is attained.

These are mixtures of still uncharacterized products. Although iCORM-3 still retains inert CO ligands,^{5, 8} iALF186 does not.¹⁴ When Mo(0) is exposed to O₂, oxidation is very fast and CO is lost, an effect first shown in low temperature matrices to lead to Mo-oxo species.⁴⁸

In fact, when we selected ALF186 as a potential experimental CORM, it was our initial contention that the final fate of pmolybdenum would be Mo^{VI}-oxo species, namely molybdate, [MoO₄]²⁻, or oligomers thereof. In contrast to its Cr^{VI} analogues that have devastating toxic and oxidizing effects, molybdate behaves as a source of natural molybdenum which has a well established biological role in a number of oxido-reductase and oxo-transferase enzymes in mammals and bacteria.⁴⁹ It is an essential metal in mammals and in human health.⁵⁰ Molybdate is a freely water soluble ion that is transported into the cells of mammals by a still unknown mechanism.¹⁰ Stable as a tetrahedral ion at alkaline pH, it starts oligomerizing as pH decreases forming isopolymolybdates [Mo_xO_{3x+1}]²⁻. The reaction can be reversed by raising the pH. In the presence of a wide variety of oxyanions [XO₄]ⁿ⁻, e.g. [PO₄]³⁻, [SiO₄]⁴⁻-heteropolyoxomolybdates are formed of which the most famous one is phosphomolybdate [PMo₁₂O₄₀]³⁻. Either molybdate or some of its oligomers^{51, 52} and polyoxomolybdates have been found to have therapeutic potential in several animal models of disease and are thus deemed potentially valuable as medicinal agents.¹¹ The analogue tetrathiomolybdate, [MoS₄]²⁻, administered as the ammonium salt, slowly hydrolyses to [MoO₄]²⁻ *in vivo*, and has been used in humans as an anti-tumor therapy without visible toxicological concerns⁵³. Its extraordinary ability to coordinate Cu ions bound to their chaperones⁵⁴ has granted [MoS₄]²⁻ Orphan Medicinal Product status by EMEA⁵⁵ for the treatment of Wilson's disease.⁵⁶

While attempting to elucidate possible interactions of ALF186 with proteins by X-ray crystallography, we showed that crystals of the model protein HEWL soaked with the compound, under normoxic conditions, led to the formation of phosphomolybdate within the protein crystal. In other words, the crystal just captured the final product of the decomposition of ALF186, which adopts a rather stable oligomeric structure known as Keggin's ion. The interaction between this polyoxometallate anion and the protein is essentially electrostatic and hydrogen bonded in nature and does not involve or form any covalent or coordination bond to the protein residues, suggesting that it may be readily mobilized as a solute. Of course, the polymerization process that leads to such polyoxometallates is highly dependent on the nature of the solution, the presence of other solutes and the pH.^{57, 58} Therefore, it is possible that under slightly different circumstances, particularly *in vivo*, other oligomers and even the monomer would have been found. In any case, our initial contention proved correct and the tendency of Mo^{VI} to form these terminal Mo=O and bridging Mo-O-Mo bonds disfavors its interaction with the surrounding biological molecules, namely the coordination to proteins.

Conclusion

The simple zerovalent molybdenum carbonyl anionic complex *fac*-[Mo(CO)₃(his)]Na, ALF186, has proven to be both a good model for the study of some fundamental interactions of metal carbonyl complexes with biological media, and a useful experimental CORM that can readily deliver free CO in biological media. Decarbonylation of ALF186 takes place following oxidation of the metal by O₂, which is the trigger for the delivery of CO, to rapidly diffuse into the blood stream after administration *in vivo*. Surprisingly, this CO delivery is extremely fast in blood both *in vitro* and *in vivo*. Thus, its effect on the rise of COHb in circulation is very predictable allowing the use of this CORM as a very useful tool to generate predefined values of COHb in the circulation under well-defined and predictable kinetics. In this setting the therapeutic effects observed *in vivo* may be correlated to the

COHb values in circulation in a close mimic of CO inhalation therapy. The reactivity of ALF186 with heme proteins and human serum albumin, its formation of $\cdot\text{OH}$ radicals upon oxidation and the generation of polyoxometallates as decomposition products in biological media are other important conclusions that improve the knowledge of fundamental bioorganometallic chemistry. Besides its use as an experimental CO delivery tool, its chemistry and biology are useful to assist the development of a second generation of drug-like CORMs, with increased stability and specific tissue targeting that enable the harnessing of the tremendous therapeutic potential of this simple diatomic gas.

Experimental section

All work involving animals performed in the Lisbon laboratories of Alfama was done according to the guidelines of the Portuguese animal protection law and derived guidelines on the ethical use of animals. All animal studies performed in the Beverly, Massachusetts, laboratories of Alfama were carried out in accordance with the Guide for the Care and Use of Laboratory Animals of the U.S. National Institutes of Health.

Chemical Synthesis

The complex *fac*-[Mo(CO)₃(histidinate)]Na (ALF186) was prepared and purified according to the literature,⁹ and characterized by FTIR, ¹H NMR, and Elemental Analysis (C,H,N). The compound was kept as a solid under a nitrogen atmosphere in the dark.

Microanalysis for CHN were performed at the Instituto de Tecnologia Química e Biológica (by C. Almeida). NMR spectra were recorded on a Bruker Avance II 400 MHz spectrometer. FTIR spectra (KBr pellets) were taken in a Unicam-Mattson 7000.

Stability studies

Room temperature stability experiments: ALF186 was aliquoted into individual vials. These were deoxygenated, closed with a rubber septum and stored inside a cardboard box to guarantee the absence of light. At chosen times samples were analyzed by ¹H NMR, FTIR, and elemental analysis. The samples stored under N₂, in the dark or in light and at room temperature were analyzed at the time of sampling, 1 week, 1.5 months and 3 months later. For samples stored in air, in the dark and at room temperature the compound was analyzed at the time of sampling and after 1 week, 1 and 2 months. No test was done under the simultaneous presence of both air and light. Photo stability experiments: These tests were carried out according to the instructions in the literature.^{19, 20}

ALF186 was aliquoted into individual vials which were deoxygenated, closed with a rubber septum and put in a clear view of a window. A 2% (w/v) aqueous quinine solution was used as a standard. The absorbance of the quinine solution was followed until it reached Abs > 0.5 (it took two months for the quinine solution to reach this value). Samples were then stored in the dark at -30°C for 8 days after which they were analyzed by ¹H NMR, FTIR and elemental analysis.

Air stability experiments: ALF186 was aliquoted into individual vials, which were closed with a punctured rubber septum and stored inside a cardboard box to guarantee the absence of light. At chosen times samples were analyzed by ¹H NMR, FTIR and elemental analysis.

Spontaneous CO release in vitro: Quantification via Gas Chromatography

The CO release assays were performed in 7.5 mL Roth[®] sample vials equipped with a magnetic stirrer inside and capped with a PTFE rubber or silicone septum and an aluminum cap. PTFE rubber septa were acquired from Sigma Aldrich[®] and silicone septa from Roth[®].

The assays were performed in the medium selected, in the dark or with light, at room temperature or 37°C, under normal atmospheric air or under N₂. The concentration of ALF186 was ≈ 10mM. Samples (250 μL) of the headspace were taken with a Gastight Hamilton[®] syringe and injected in a Thermo Finnigan Trace GC equipped with a CTR1 column from Alltech[™] and a Thermal Conductivity Detector. The column was inside an oven at 36 °C, and the GC was operated at a constant pressure mode (111 KPa) with He as carrier and reference gas with a 30 mL/min flow. Detector was set at constant temperature (150°C) and the filament at 250°C. Injections were made through a packed column injector (PKD) set at 47 °C and 111 KPa. CO was quantified using a calibration curve recorded prior to the reaction course. Standards were prepared by injecting 250 μL increments of CO up to a final total amount of 2 mL of pure CO gas (Carbon Monoxide 3.7, purity. ≥99.997%) in closed vials with 2 mL of distilled water, using a Gastight Hamilton[®] syringe. Gas samples (250 μL) were taken and analyzed by GC.

Redox reactions with heme proteins

In the following experiments ALF186 solutions were prepared in degassed PBS buffer at pH 7.4 and added to the protein solutions prepared in the same buffer under normoxic conditions.

Reaction between ALF186 and cytochrome *c*: a solution of cytochrome *c* (5 μM) from horse heart muscle (*Sigma Aldrich*) was mixed with the ALF186 (50 μM) in PBS buffer at pH 7.4. The UV-Vis absorbance spectrum was recorded immediately after mixing the sample, using quartz cuvettes (b=10mm). As a control, CO gas was bubbled into a cytochrome *c* solution for 20 min and no changes were observed in the spectrum.

Reaction between ALF186 and myoglobin: a solution of myoglobin (11 μM) from equine skeletal muscle (95–100%, essentially salt free lyophilized powder from *Sigma*) was prepared by dissolving the protein in PBS buffer at pH 7.4 and ALF186 (50 μM) was added in PBS buffer at pH 7.4. The UV-Vis absorbance spectrum was recorded immediately after mixing the sample, using quartz cuvettes (b=10mm).

Reaction between ALF186 and hemoglobin: A solution of bovine hemoglobin (5 μM) was prepared by dissolving the protein in PBS buffer at pH 7.4 and ALF186 (50 μM) was added in PBS buffer at pH 7.4. The UV-Vis absorbance spectrum was recorded immediately after mixing the species, using quartz cuvettes (b=10mm).

CO release in blood (in vitro)

A solution of ALF186 was prepared in PBS buffer at pH 7.4 and 50 μL were added to 1 mL of sheep whole blood in Alsevers solution (Innovative Research cat n° IR1-020N) and incubated at 37°C. Samples were kept inside closed plastic culture tubes with closures (5 mL; 12×75 mm) and analyzed over time in the oximeter (Avoximeter 4000 from A-vox Instruments Inc.; disposable cuvettes for Avoximeter 4000 from A-vox Instruments Inc.) to follow the raise in COHb levels.

The amount of CO liberated was calculated based on the amount of compound initially added, total amount of Hemoglobin and %COHb (both given by the oximeter). The compound was tested in a concentration calculated in order to mimic relevant *in vivo* doses. Assuming a 20 g mouse with 8% blood volume (1.6 mL), 10 mg/kg correspond to 0.2 mg of compound/animal, therefore 0.2mg/1.6 mL of blood, which corresponds to a final concentration of 0.125 mg/mL of ALF186. Control spectra of the free medium were always recorded.

Hemolytic index

Red Blood Cells (RBC) obtained upon centrifugation of sheep whole blood (in Alsevers' solution; Innovative Research cat n° IR1-020N) were used in the assays to evaluate the potential of ALF186 to induce RBC hemolysis.

A 2% RBC suspension in PBS (100 μ L) was distributed in the wells of a 96-well plate. The effect of ALF186 was evaluated in concentrations between 0.0078 to 1 mg/mL. A 2 mg/mL solution of ALF186 in PBS was prepared followed by $\frac{1}{2}$ serial dilutions in PBS. ALF186 prepared solutions were added (100 μ L) to the RBC suspension. The ALF186-RBC suspension was then incubated for 1h at 37°C. As a positive control of the experiment, a 2% RBC solution in water was prepared.

The plate was then centrifuged and the absorbance of the supernatant was measured at 550 nm in a microplate reader (Bio-Rad). The Hemolytic Index (HI) was determined using the following formula:

$$\text{HI (\%)} = \frac{\text{OD (ALF186 sample)} - \text{OD (ALF186 reference)}}{\text{OD (positive control)} - \text{OD (negative control)}} \times 100$$

OD (ALF186 reference) – OD of the corresponding ALF186 solution (endogenous abs).

OD (positive control) – OD of the solution obtained by lysis of the RBC (1% RBC)

OD (negative control) – OD of the 1% RBC suspension in PBS after centrifugation

A hemolytic index above 10% indicates hemolysis.

Interaction with Human Serum Albumin

A CORM stock solution was prepared in PBS buffer at pH 7.4. An aliquot from this solution was added to a cuvette in order to obtain a 250 μ M final concentration and PBS buffer at pH7.4 added to perform 1 mL total volume. Absorbance spectra were recorded between 250 nm and 800 nm with 10 min interval in a Perkin Elmer Lambda35 spectrophotometer.

A similar experiment was performed but where HSA (50 μ M final concentration) in PBS buffer at pH 7.4 was added to the solution. Absorbance spectra were recorded between 250 nm and 800 nm with 10 min interval in a Perkin Elmer Lambda35 spectrophotometer.

For the experiments under N_2 , the PBS solution was bubbled with N_2 for 1h and all the solutions prepared inside Schlenk tubes.

Interaction with HEWL and X-ray Crystallography

Crystals of hen egg white lysozyme (HEWL) from Merck were grown at 20°C using the hanging drop vapor diffusion method. The best crystallization conditions were 2–10% (m/v) NaCl and 0.1 M acetate buffer pH 4.5 (the protein:well solution ratio in the drop was 1:1 with the final drop volume of 4 μ L) using a protein stock concentration of ~50 mg/mL. Crystals of 0.2 mm size appeared within 24 h and were stabilized overnight with a harvesting solution containing 12% (m/v) NaCl in the same buffer. A solution of ALF186 was prepared in water and added to the crystal drops to a final concentration of 0.1 M. After 24 h, crystals had turned blue and were flash frozen using Paratone oil as cryoprotector.

Diffraction data were collected at beam line ID14–1 at the ESRF (Grenoble, France) using a ADSC Q210 CCD detector. The data set was processed and scaled using MOSFLM⁵⁹ and

SCALA from the CCP4 suite.⁶⁰ Details of data collections and processing are presented in Table 2.

The structure was solved by rigid body refinement in Refmac 5,⁶¹ using pdb entry 193L as a model. Data in the resolution range 30.38-1.67 Å were used for refinement. Iterative model building with COOT guided by $2mF_0-DF_c$ and mF_0-DF_c maps, together with restrained refinement in REFMAC resulted in good final model (as judged by the validation tools in COOT⁶²). The final model contains amino acid residues 1–129, a $[\text{PMo}_{12}\text{O}_{40}]^{3-}$ cluster, a Na^+ and a Cl^- ion from the crystallization solution. Oxygen atoms of the $[\text{PMo}_{12}\text{O}_{40}]^{3-}$ were not included in the final coordinate. Refinement statistics are summarized in Table 2. The coordinates and structure factor have been deposited in PDB with accession number 4B1A.

Cytotoxicity

The cytotoxicity of ALF186 was evaluated in three different cell lines: murine macrophage RAW264.7 (ECACC 91062702); porcine kidney epithelial LLC-PK1 (ECACC 86121112); and human hepatoma HepG2 (ECACC 85011430).

For each cell line a cell suspension of approximately 1.5×10^6 cells/mL in culture medium [DMEM (GIBCO, Cat. No. 41966) for RAW264.7 and LLC-PK1; or MEM (GIBCO, Cat. No. 41090) for HepG2] supplemented with 10% FBS (GIBCO, Cat. No. 10500) was seeded (100 μL) into the wells of a 96-well plate. The cytotoxicity was evaluated by incubating the cells for 24h at 37°C, 5% CO_2 , in the presence of 1, 3, 10, 30 and 100 μM of ALF186.

Cell survival was determined using the colorimetric MTT assay, which involves the metabolization of the 3-(4,5-dimethylthiazol-2-yl)-2,5-diphenyltetrazolium bromide (MTT), a yellow tetrazole, into the purple formazan crystals.

After 24h, the culture medium was removed and replaced by fresh medium supplemented with 1 mg/mL MTT. The cells were incubated for 1h at 37°C, 5% CO_2 . The formazan crystals produced were solubilized with DMSO and the absorbance of the final solution was determined at 550 nm (BioRad microplate reader).

Toxicity is indicated by a reduced purple color compared to the control.

CO release in vivo

Balb/C mice from Charles River (6–8 weeks old) were treated with ALF186 (20 or 40 mg/kg, i.p.) dissolved in PEG300/water (1:4). Blood samples were collected after 2, 5, 10, 30, 60, 120 and 180 min and COHb was determined using an AVOXimeter 4000 (A-VOX Systems, Inc., San Antonio, TX, USA). Percent COHb at each time point is the average of 3 different mice.

Balb/C mice (6–8 weeks old) were treated orally with ALF186 by gavage at a dose of 500 mg/kg in PEG300:water (1:4). Blood samples were collected after 2, 5, 10, 30 and 60 min, and COHb was determined using an AVOXimeter 4000. Percent COHb at each time point is the average of 3 different mice.

Hemodynamic Measurements

Effect of ALF 186 on blood pressure was measured by cannulating the femoral arteries of C57BL/6 mice 8–9 weeks of age. Ketamine 100mg/kg and Xylazine 20mg/kg were used as anesthetic due to its limited effects on respiration and cardiac output. After mice were cannulated an initial blood pressure was taken using an AD Instrument blood pressure

monitoring system. The average baseline blood pressure in an anesthetized animal ranged between 75–80 mmHg. Since both femoral arteries were cannulated it was possible to continuously monitor blood pressure and measure COHb throughout the experiment, which lasted up to 120 min. ALF186 and the inactive ALF186 at 20mg/kg were injected i.p. The inactive form of ALF186 was created by allowing the compound to incubate in solution at room temperature for at least 24h. During this time period, the compound turned from yellow to brown indicating a loss of CO. After injection, blood pressure and COHb levels were measured every 20 min. Similar experiments were done with inhaled CO (iCO) where mice were exposed to a concentration of 250 ppm CO continuously throughout the experiment. Air control animals were treated exactly the same as the iCO animals but under normal atmosphere.

Supplementary Material

Refer to Web version on PubMed Central for supplementary material.

Acknowledgments

The authors would like to acknowledge Fundação para a Ciência e Tecnologia for funding through grant no. PEST-C/EQB/LA0006/2011, PTDC/QUI-BIQ/117799/2010 and post-doc grant SFRH/BPD/30142/2006. The nuclear magnetic resonance spectrometers are part of the National NMR Network and were purchased in the framework of the National Program for Scientific Re-equipment, contract REDE/1517/RMN/2005, with funds from POCI 2010 (FEDER) and Fundação para a Ciência e a Tecnologia. We thank the Julie Henry Fund of the Transplant Institute at the BIDMC for their continued support. LEO is supported by NIH grants 5R01GM088666 and R56AI092272. The authors thank FCT for the grants SFRH/BPD/70163/2010 (A.C.C.) and SFRH/BPD/20655/2004 (P.M.R.).

Abbreviations

rt	room temperature
NMR	nuclear magnetic resonance
FTIR	Fourier transform infrared spectroscopy
RPMI	Roswell Park Memorial Institute medium
PBS	phosphate buffered solution
BSA	bovine serum albumin
COHb	carboxyhemoglobin
COMb	carboxymyoglobin
cyt	cytochrome
GC	gas chromatography
Hb	hemoglobin
HEWL	hen egg white lysozyme
his	histidinate
HSA	human serum albumin
i. p	intraperitoneal
i.v	intravenous
p.o	<i>per os</i> , orally
RBC	red blood cell

MABP mean arterial blood pressure

References

1. Mann, BE. *Top Organomet Chem.* Jaouen, G.; Metzler-Nolte, N., editors. Springer; Berlin: 2010. p. 247-285.
2. Motterlini R, Otterbein LE. *Nat Rev Drug Discov.* 2010; 9:728–743. [PubMed: 20811383]
3. Romão CC, Blättler WA, Seixas JD, Bernardes GJL. *Chem Soc Rev.* 2012; 41:3571–3583. [PubMed: 22349541]
4. Motterlini R, Clark J, Foresti R, Sarathchandra P, Mann B, Green C. *Circ Res.* 2002; 90:E17–E24. [PubMed: 11834719]
5. Clark J, Naughton P, Shurey S, Green C, Johnson T, Mann B, Foresti R, Motterlini R. *Circ Res.* 2003; 93:E2–E8. [PubMed: 12842916]
6. Guo Y, Stein AB, Wu W-J, Tan W, Zhu X, Li Q-H, Dawn B, Motterlini R, Bolli R. *Am J Physiol Heart Circ Physiol.* 2004; 286:H1649–1653. [PubMed: 14704226]
7. Wang G, Hamid T, Keith RJ, Zhou G, Partridge CR, Xiang X, Kingery JR, Lewis RK, Li Q, Rokosh DG, Ford R, Spinale FG, Riggs DW, Srivastava S, Bhatnagar A, Bolli R, Prabhu SD. *Circ Res.* 2010; 121:1912–1925.
8. Santos-Silva T, Mukhopadhyay A, Seixas JD, Bernardes GJL, Romão CC, Romão MJ. *J Am Chem Soc.* 2011; 133:1192–1195. [PubMed: 21204537]
9. Beck W, Petri W, Meder J. *J Organomet Chem.* 1980; 191:73–77.
10. Mendel RR. *Biofactors.* 2009; 35:429–434. [PubMed: 19623604]
11. Rhule J, Hill C, Judd D. *Chem Rev.* 1998; 98:327–357. [PubMed: 11851509]
12. Barceloux D. *J Toxicol Clin Toxic.* 2000; 38:813–813.
13. Rodrigues, SS.; Seixas, JD.; Guerreiro, B.; Pereira, NMP.; Romão, CC.; Haas, WE.; Gonçalves, IMS. US 2011/0038955 A1.
14. Sheikh SZ, Hegazi RA, Kobayashi T, Onyiah JC, Russo SM, Matsuoka K, Sepúlveda AR, Li F, Otterbein LE, Plevy SE. *J Immunology.* 2011; 186:5506–5513. [PubMed: 21444764]
15. Schallner, N.; Otterbein, LE.; Romão, CC.; Rodrigues, SS.; Loop, T.; Goebble, U. 7th Int. Congress on Heme Oxygenases and Related Enzymes; 2012.
16. van Staveren D, Metzner-Nolte N. *Chem Commun.* 2002:1406–1407.
17. Mohr F, Niesel J, Schatzschneider U, Lehman Z. *Z Anorg Allg Chem.* 2012; 638:543–546.
18. Schatzschneider U. *Inorg Chim Acta.* 2011; 374:19–23.
19. ICH Harmonized Tripartite Guideline Stability Testing: Photostability Testing of New Drug Substances and Products, Q1B. 1996.
20. Christensen KL, Christensen JO, Frokjaer S, Langballe P, Hansen LL. *Eur J Pharm Sci.* 2000; 9:317–321. [PubMed: 10594390]
21. Buehler PW, Alayash AI. *Antiox Redox Signaling.* 2005; 7:1755–1760.
22. McLean S, Mann BE, Poole RK. *Anal Biochem.* 2012:1–21.
23. Kragh-Hansen U. *Pharmacol Rev.* 1981; 33:17–53. [PubMed: 7027277]
24. Fehske KJ, Müller WE, Wollert U. *Biochem Pharmacol.* 1981; 30:687–692. [PubMed: 7018498]
25. Liu M, Lim ZJ, Gwee YY, Levina A, Lay PA. *Angew Chem-Int Ed Eng.* 2010; 49:1661–1664.
26. Almo SC, Bonanno JB, Sauder JM, Emtage S, Dilorenzo TP, Malashkevich V, Wasserman SR, Swaminathan S, Eswaramoorthy S, Agarwal R, Kumaran D, Madegowda M, Ragumani S, Patskovsky Y, Alvarado J, Ramagopal UA, Faber-Barata J, Chance MR, Sali A, Fiser A, Zhang Z-y, Lawrence DS, Burley SK. *J Struct Funct Genom.* 2007; 8:121–140.
27. Reinelt S. *J Biol Chem.* 2003; 278:39189–39196. [PubMed: 12867417]
28. Allen F. *Acta Crystallogr, Sect B: Struct Sci.* 2002; 58:380–388.
29. Darensbourg D, Atnip E, Klausmeyer K, Reibenspies J. *Inorg Chem.* 1994; 33:5230–5237.

30. Darensbourg D, Klausmeyer K, Reibenspies J. *Inorg Chem.* 1996; 35:1535–1539. [PubMed: 11666369]
31. Wegiel B, Gallo DJ, Raman KG, Karlsson JM, Ozanich B, Chin BY, Tzeng E, Ahmad S, Ahmed A, Baty CJ, Otterbein LE. *Cir Res.* 2010; 121:537–548.
32. Marazioti A, Bucci M, Coletta C, Vellecco V, Baskaran P, Szabó C, Cirino G, Marques AR, Guerreiro B, Gonçalves AML, Seixas JD, Beuve A, Romão CC, Papapetropoulos A. *Arterioscler, Thromb, Vasc Biol.* 2011; 31:2570–2576. [PubMed: 21836072]
33. Sawle P, Foresti R, Mann BE, Johnson TR, Green CJ, Motterlini R. *Br J Pharmacol.* 2005; 145:453–460.
34. Foresti R, Hammad J, Clark JE, Johnson TR, Mann BE, Friebe A, Green CJ, Motterlini R. *Br J Pharmacol.* 2004; 142:453–460. [PubMed: 15148243]
35. Seixas, JD. Ph D Dissertation. Instituto Tecnologia Química e Biológica; 2011.
36. Tavares AFN, Teixeira M, Romão CC, Seixas JD, Nobre LS, Saraiva LM. *J Biol Chem.* 2011; 286:26708–26717. [PubMed: 21646348]
37. Zuckerbraun BS, Chin BY, Bilban M, de Costa d'Avila J, Rao J, Billiar TR, Otterbein LE. *FASEB J.* 2007; 21:1099–1106. [PubMed: 17264172]
38. Santos-Silva T, Mukhopadhyay A, Seixas JD, Bernardes GJL, Romão CC, Romão MJ. *Curr Med Chem.* 2011; 18:3361–3366. [PubMed: 21728965]
39. Pena AC, Penacho N, Mâncio-Silva L, Neres R, Seixas JD, Fernandes AC, Romão CC, Mota MM, Bernardes GJL, Pamplona A. *Antimicrob Agents Chemother.* 2012; 56:1281–1290. [PubMed: 22155828]
40. Santos M, Seixas J, Coelho A, Mukhopadhyay A, Reis P, Romão MJ, Romão CC, Santos-Silva T. *J Inorg Biochem.* 2012; 7:327–337.
41. Zhang Y, Wilcox DE. *J Biol Inorg Chem.* 2002; 7:327–337. [PubMed: 11935357]
42. Storr T, Thompson K, Orvig C. *Chem Soc Rev.* 2006; 35:534–544. [PubMed: 16729147]
43. Thompson K, Orvig C. *Science.* 2003; 300:936–939. [PubMed: 12738851]
44. Blanco-Rodriguez A, Busby M, Gradinaru C, Crane B, Di Bilio A, Matousek P, Towrie M, Leigh B, Richards J, Vlček A, Gray H. *J Am Chem Soc.* 2006; 128:4365–4370. [PubMed: 16569013]
45. Razavet M, Artero V, Cavazza C, Oudart Y, Lebrun C, Fontecilla-Camps JC, Fontecave M. *Chem Commun.* 2007:2805–2807.
46. Binkley SL, Ziegler CJ, Herrick RS, Rowlett RS. *Chem Commun.* 2010; 46:1203–1205.
47. Gonzalez MA, Fry NL, Burt R, Davda R, Hobbs A, Mascharak PK. *Inorg Chem.* 2011; 50:3127–3134. [PubMed: 21384844]
48. Almond M, Crayston J, Downs A, Poliakoff M, Turner J. *Inorg Chem.* 1986; 25:19–25.
49. Romão MJ. *Dalton Trans.* 2009:4053–4068. [PubMed: 19452052]
50. Jelikić-Stankov M, Uskoković-Marković S, Holclajtner-Antunović I, Todorović M, Djurdjević P. *J Trace Elements Med Biol.* 2007; 21:8–16.
51. Eidi A, Eidi M, Al-Ebrahim M, Rohani AH, Mortazavi P. *J Trace Elements Med Biol.* 2011; 25:67–71.
52. Thompson K, Chiles J, Yuen V, Tse J, McNeill J, Orvig C. *Journal Of Inorg Biochem.* 2004; 98:683–690. [PubMed: 15134913]
53. Hassouneh B, Islam M, Nagel T, Pan Q, Merajver S, Teknos T. *Mol Cancer Ther.* 2007; 6:1039. [PubMed: 17363496]
54. Alvarez HM, Xue Y, Robinson CD, Canalizo-Hernandez MA, Marvin RG, Kelly RA, Mondragon A, Penner-Hahn JE, O'Halloran TV. *Science.* 2010; 327:331–334. [PubMed: 19965379]
55. EMEA. Pre-authorisation Evaluation of Medicines for Human Use EMEA/COMP/82161/2008.
56. Brewer GJ, Askari F, Dick RB, Sitterly J, Fink JK, Carlson M, Kluin KJ, Lorincz MT. *Transl Res.* 2009; 154:70–77. [PubMed: 19595438]
57. Vilà-Nadal L, Wilson EF, Miras HN, Rodríguez-Fortea A, Cronin L, Poblet JM. *Inorg Chem.* 2011; 50:7811–7819. [PubMed: 21766888]
58. Walanda DK, Burns RC, Lawrance GA, von Nagy-Felsobuki EI. *Dalton Trans.* 1999; 311:322.
59. Leslie, A. Joint CCP4+ ESF-EAMCB Newsletter on Protein Crystallography. Warrington: 1992.

60. Kabsch W. *Acta Crystallogr, Sect A: Found Crystallogr.* 1978; 34:827–828.
61. Murshudov GN, Vagin AA, Dodson EJ. *Acta Crystallogr D Biol Crystallogr.* 1997; 53:240–255. [PubMed: 15299926]
62. Emsley P, Cowtan K. *Acta Crystallogr, Sect D: Biol Crystallogr.* 2004; 60:2126–2132. [PubMed: 15572765]

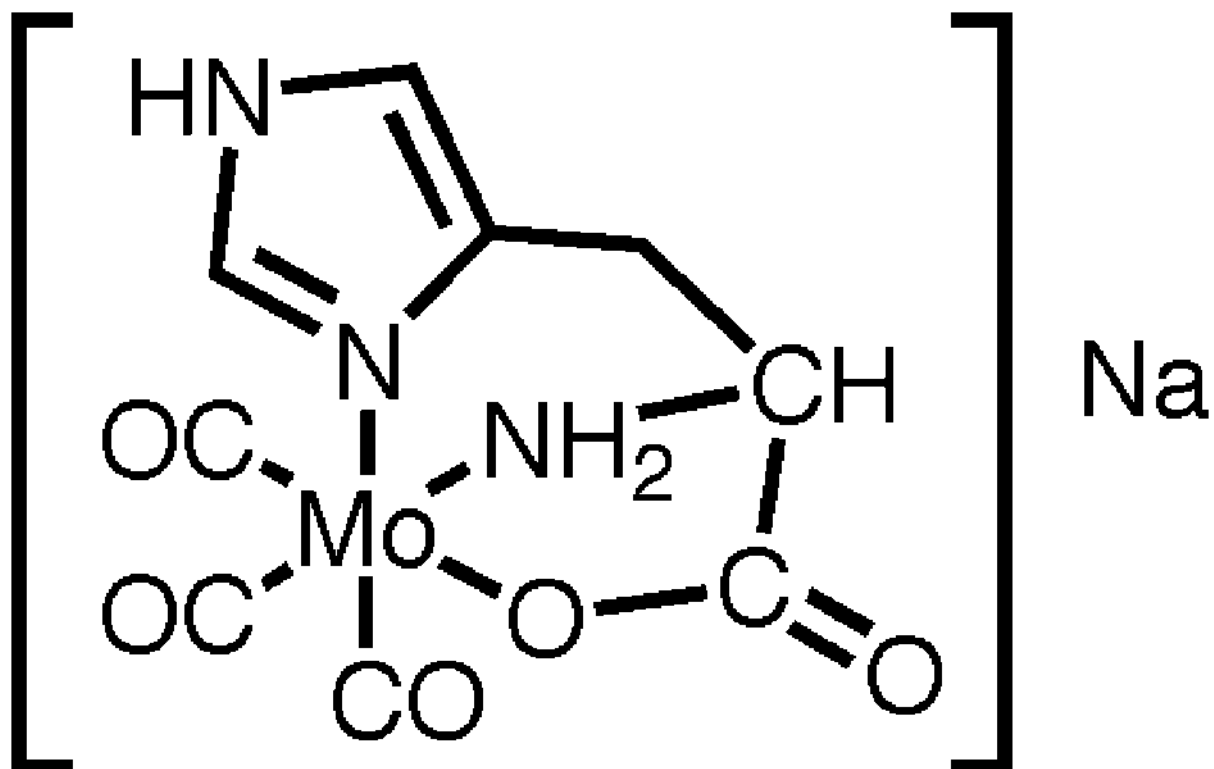


Figure 1.
Structure of ALF186

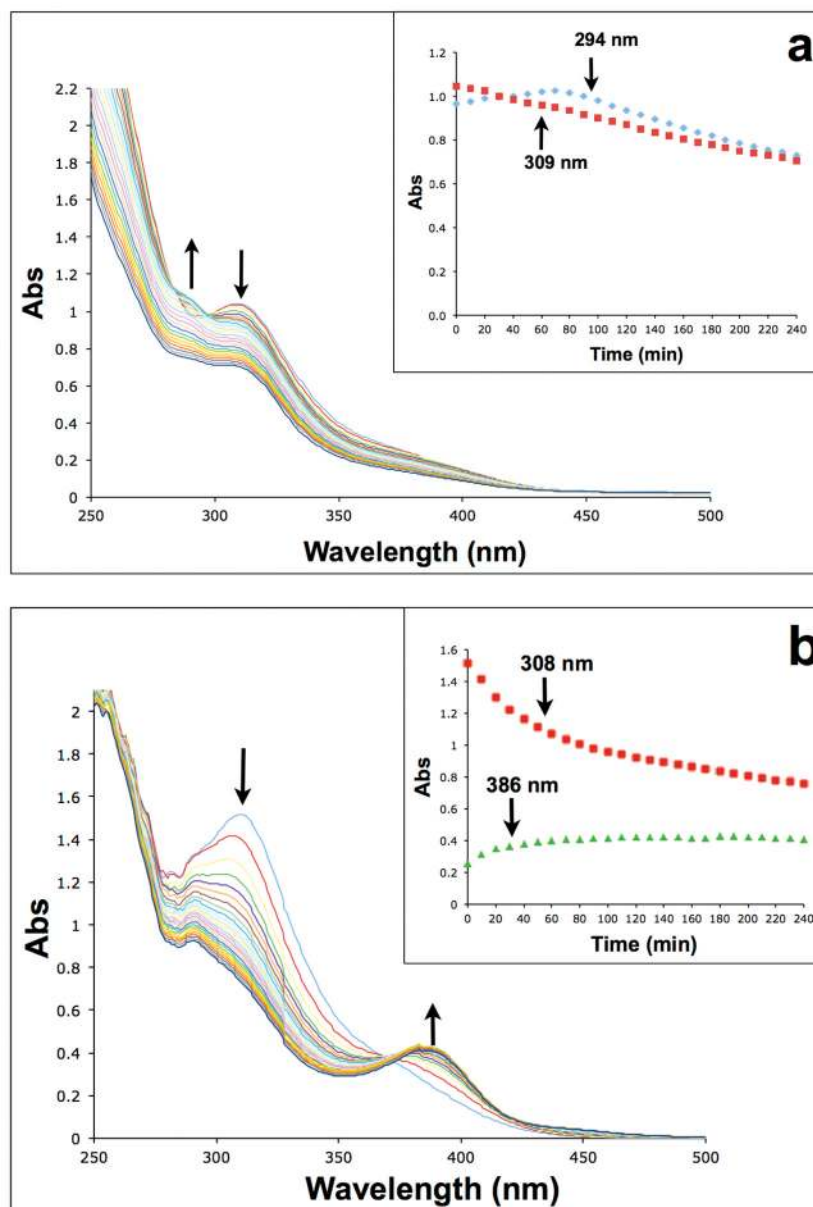


Figure 2. Time evolution of UV-Vis absorption spectrum of ALF186 in PBS buffer at pH7.4 at rt under aerobic conditions: a) decay in absorbance measured at 294 nm and 309 nm with ALF186 alone (250 μM). b) Decay in absorbance measured at 308 nm and 386 nm with ALF186 and HSA (250 μM and 50 μM, respectively; HSA spectrum subtracted). The variation of the absorbance with time is given in the insets.

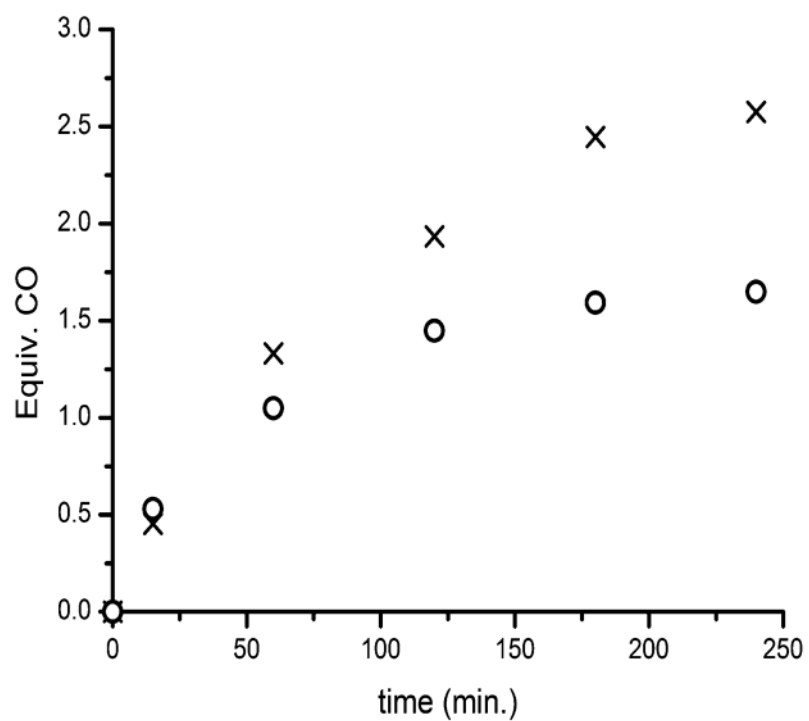


Figure 3. Plot of equivalents of CO released versus time from a solution of pure ALF186 in PBS buffer at pH7.4 (X) and from a solution of a 5:1 molar ratio mixture of ALF186:BSA (O). Experiments done at rt with GC-TCD detection of CO. The solution and headspace volume, as well as the mass and concentration of ALF186 (10mM), was the same in both experiments. The amount of CO₂ released after 4h is only 0.04 equivalents.

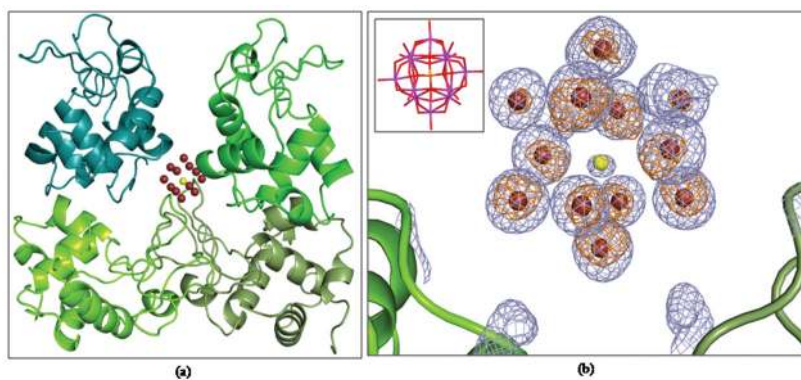


Figure 4. Structure of polyoxomolybdate cluster $[\text{PMo}_{12}\text{O}_{40}]^{3-}$ hydrogen bonded to HEWL. For clarity, only molybdenum (brown) and phosphorus (yellow) atoms are shown; (a) cartoon representation of the crystal packing with the Keggin's ion surrounded by four protein molecules (b) $2mF_o-DF_c$ maps (contoured at 1.5σ , in blue) and anomalous peaks (contoured at 2.5σ , in yellow) obtained after model building and refinement. In the inset is a representation of the structure of the Keggin's ion from Cambridge structural database.²⁸

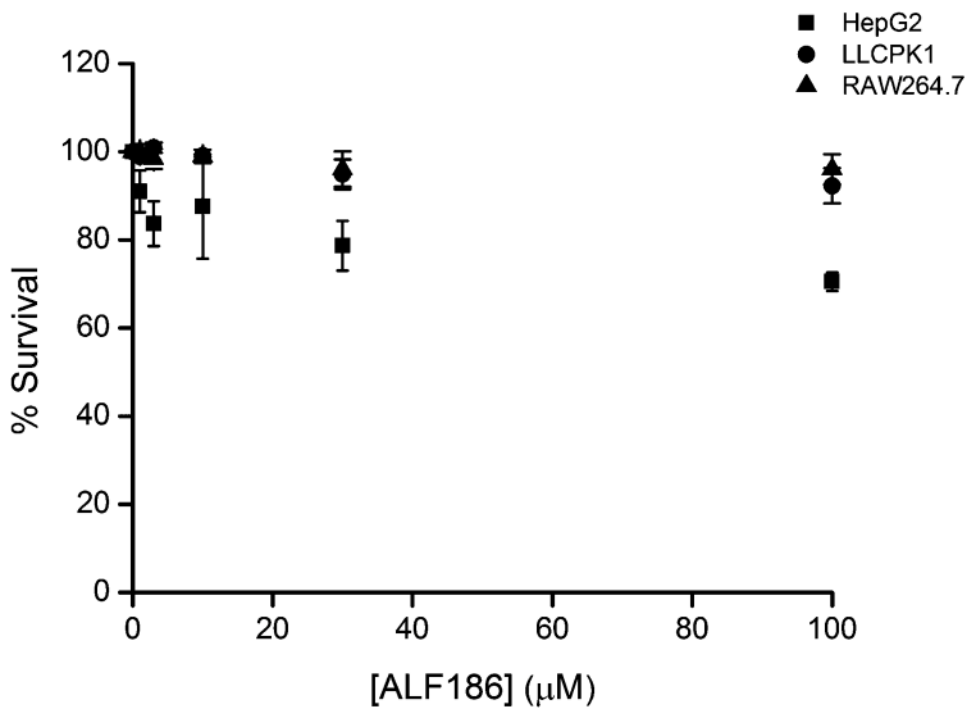


Figure 5. Toxicity of ALF186 *in vitro*: HepG2, LLC-PK1 and RAW264.7 cell lines. Cells were incubated for 24h (37°C, 5% CO₂) in the presence of ALF186 at concentrations up to 100 μM . The percentage of cell survival was calculated considering 100% survival for control cells.

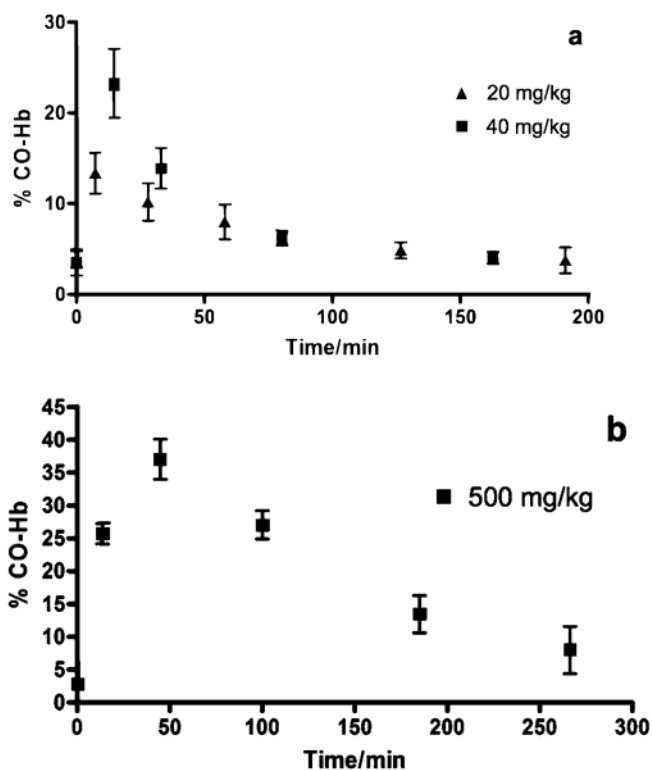


Figure 6.

a) %COHb levels after i.p. administration of 20 mg/kg and 40 mg/kg of ALF186 in Balb/C mice, in PEG300/water (1:4). Average of three mice for each dose **b)** %COHb levels after oral administration of 500 mg/kg of ALF186 in Balb/C mice, in PEG300/water (1:4). %COHb at each time point is the average of three different mice.

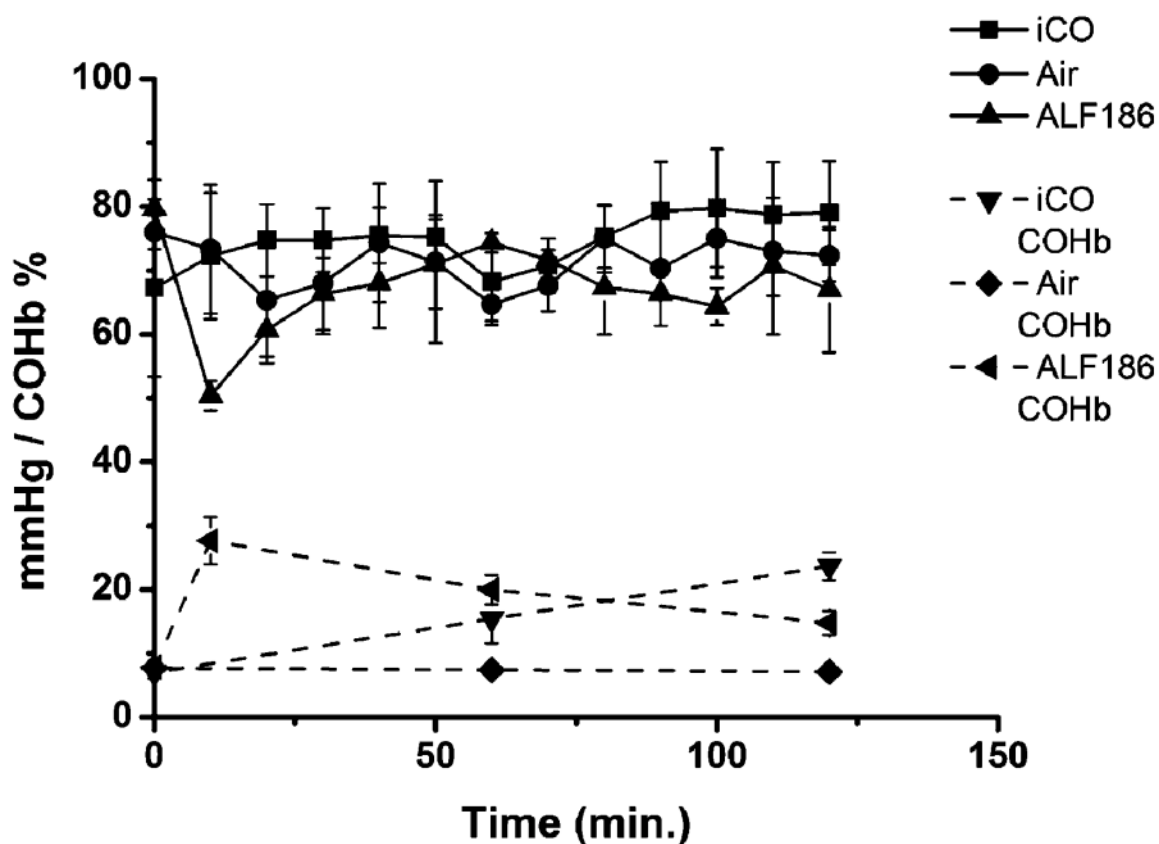


Figure 7.

Bottom plot (dashed lines): time evolution of the % COHb levels in mice treated with inhaled CO (250 ppm) and with ALF186 (20 mg/kg, i.p. administration). Top plot (solid lines): time evolution of the mean arterial blood pressure (mmHg) for mice treated with inhaled CO (iCO) as in the bottom plot. Both plots include the control values for mice breathing normal air. These are similar to the controls for i.p. administration of inactivated ALF186 (not shown).

Table 1

Oximetry results and calculated equiv. CO after incubation of ALF186 in sheep blood (121.9 $\mu\text{g/ml}$; 342 μM).

Time (min)	Total Hb (g/dL)	% O ₂ -Hb	% COHb	%met-Hb	Calculated Equiv. CO
0	7.7	76.5	21.3	0.0	2.98
2	7.3	76.2	21.6	0.0	2.86
4	7.3	76.8	21.7	0.0	2.88

Table 2

Data collection and refinement statistics

Dataset	Lys-186
X-ray source	ID14-1 (ESRF)
Crystal data	
Space group	$P4_32_12$
Unit cell parameters (Å)	$a=77.96$
	$b=77.96$
	$c=36.41$
Molecules per ASU	1
Mosaicity	0.83
Matthews coefficient (Å ³ Da ⁻¹)	1.91
Solvent content (%)	35.5
Max. resolution (Å)	1.67
Data collection and processing	
Wavelength (Å)	0.934
Resolution limits (Å)	30.38 – 1.67 (1.76 – 1.67)
No. of observed reflections	182638 (25983)
No. of unique reflections	13544 (1940)
Redundancy	13.5 (13.4)
R_{pim}	0.015 (0.105)
Completeness (%)	99.6 (100)
$\langle I/\sigma \rangle$	29.7 (6.4)
Refinement statistics	
Resolution (Å)	30.38-1.67
Reflections used	12793
R_{work} (%)	21.50
R_{free}^a (%)	26.66
Number of water molecules	104
Ramachandranplot ^b :	
Residues other than Gly and Pro in:	
Most favored regions (number)	124
Additional allowed regions (number))	5
Disallowed regions (number)	0
PDB code	4B1A

^a R_{free} is calculated for a randomly chosen 5% of the reflections for each dataset.

^b Calculated using COOT validation.